Effects of Mn, Si, and Purity on the Design of 3.5NiCrMoV, 1CrMoV, and 2.25Cr-1Mo Bainitic Alloy Steels

R.L. BODNAR, T. OHHASHI, and R.I. JAFFEE

Three high-temperature bainitic alloy steels were evaluated in the laboratory to determine the effects of Mn, Si, and impurities (*i.e.*, S, P, Sn, As, and Sb) on microstructure and mechanical properties. The alloy steels were 3.5NiCrMoV and CrMoV, which are used for turbine rotors, and 2.25Cr-1Mo, which is used in pressure vessel applications. The important effects of Mn, Si, and impurities, which should control the design of these high-temperature bainitic steels, are presented. Key results are used to illustrate the influence of these variables on cleanliness, overheating, austenitizing, hardenability, tempering, ductility, toughness, temper embrittlement, creep rupture, and low-cycle fatigue. Low levels of Mn, Si, and impurities not only result in improved temper embrittlement resistance in these steels but also lead to an improvement in creep rupture properties (*i.e.*, improved strength and ductility). These results have produced some general guidelines for the design of high-temperature bainitic steels. Examples illustrating the implementation of the results and the effectiveness of the design guidelines are provided. Largely based on the benefits shown by this work, a high-purity 3.5NiCrMoV steel, which is essentially free of Mn, Si, and impurities, has been developed and is already being used commercially.

I. INTRODUCTION

OVER the past thirty years, it has been well established that both Mn and Si contribute to the temper embrittlement susceptibility of alloy steels.[1-25] The respective mechanisms by which these elements contribute to temper embrittlement, however, continue to evolve. Several researchers[6,11-14,17-20,24,25] have shown that manganese promotes the segregation of P to prior-austenite grain boundaries, thus reducing grain boundary cohesive strength. In recent years, it has been established that manganese by itself is a potent embrittling element which reduces intergranular fracture strength.[24,25] The role of Si is more complex. In Ni-bearing steels, Si behaves as an embrittling element and cosegregates with Ni to prior-austenite grain boundaries.[9] In Ni-free or low-Ni steels, the role of silicon is less clear, but it is believed to promote the segregation of P to prior-austenite grain boundaries.[11,13,17,19]

Temper embrittlement susceptibility is often assessed by measuring the shift in the 50 pct Charpy fracture appearance transition temperature (Δ50 pct FATT) between a nonembrittled and a potentially embrittled condition, *e.g.*, water quenched from the tempering temperature and slow cooled (or "step cooled") through the temper embrittling regime (575 °C to 350 °C) from the tempering temperature, respectively. Temper embrittlement susceptibility can also be assessed by measuring the Δ50 pct FATT between the water quenched from the tempering temperature and isothermally aged in the temper embrittling regime conditions. Watanabe and

Murakami[26] have correlated this Δ50 pct FATT with the so-called "*J* factor" for both 2.25Cr-1Mo and 3.5NiCrMoV steels, as shown in Figure 1. The *J* factor is expressed as

$$J = (\text{pct Mn} + \text{pct Si}) \times (\text{pct P} + \text{pct Sn}) \times 10^4 \quad [1]$$

where Mn, Si, P, and Sn are in weight percent. The tendency for temper embrittlement increases with increasing levels of Mn, Si, P, and Sn. From Figure 1, which also contains 2.25Cr-1Mo data from other researchers,[27,28,29] it is evident that *J* factors of <100 and <10 are required to minimize temper embrittlement (*i.e.*, Δ50 pct FATT < 25 °C) in the 2.25Cr-1Mo and 3.5NiCrMoV steels, respectively.

In addition to providing resistance to temper embrittlement, there are other benefits from low-Si alloy steels, *viz.*, (a) reduced A-type segregation in large ingots,[30-40] (b) improved cleanliness through the reduction of oxide and silicate types of inclusions, and (c) improved dehydrogenation during stream degassing.[30,34,37] In addition, Swaminathan *et al.*[41] found improved toughness and creep rupture ductility in a CrMoV rotor forging when the Si content was reduced from 0.25 to 0.05 pct. Based on temper embrittlement work, NiCrMoV rotor steels have been produced by vacuum carbon deoxidation (low-silicon practice) since the early 1960's. Because of the extensive research in the area of temper embrittlement and the additional advantages which have been magnified in recent years, other alloy steels such as 2.25Cr-1Mo and CrMoV are now also being produced routinely with low-Si levels, *e.g.*, <10 pct.

The attractive feature of both Mn and Si is that they can be controlled by standard steelmaking techniques,[42,43] thus possibly allowing commercial-purity residual element levels such as 0.005 to 0.010 pct P, 0.008 to 0.012 pct Sn, 0.006 to 0.010 pct As, and 0.0010 to 0.0020 pct Sb, all of which are known to contribute to temper embrittlement, to be tolerated. Developments in ladle metallurgy over the past ten years have allowed the

R.L. BODNAR, Senior Research Engineer, is with the Bethlehem Steel Corporation, Homer Research Laboratories, Building G, Bethlehem, PA 18016. T. OHHASHI was formerly Research Scientist, Japan Steel Works, Ltd., Muroran Research Laboratory, 4 Chatsumachi, Muroran, 051 Japan. R.I. JAFFEE, Senior Technical Advisor, is with the Electric Power Research Institute, 3412 Hillview Avenue, P.O. Box 10412, Palo Alto, CA 94303.
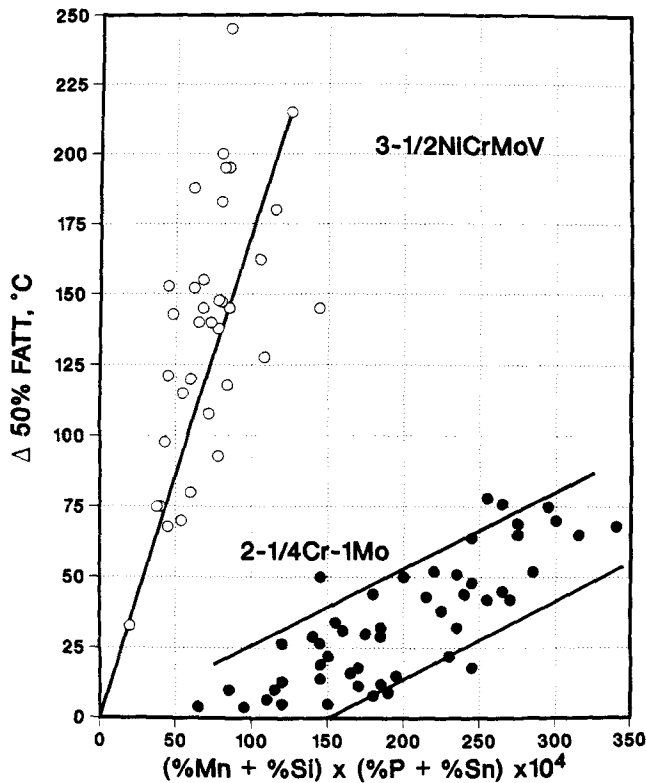Manuscript submitted July 20, 1988.

Fig. 1 — Influence of the J factor on the shift in transition temperature between water-quenched and step-cooled (from the tempering temperature) conditions for both 3.5NiCrMoV and 2.25Cr-1Mo steels.

production of clean steels with lower levels of P and S, e.g., <0.004 and <0.003 pct, respectively.[22] However, since Sn, As, and Sb cannot be reduced easily through ladle metallurgy, these elements must be con-

trolled through judicious scrap selection or the use of basic oxygen furnace starting metal.

Recently, a systematic study sponsored by the Electric Power Research Institute (EPRI) was conducted to determine the influences of Mn, Si, and impurity elements (S, P, Sn, As, and Sb) on the microstructure and mechanical properties of bainitic alloy steels for high-temperature application, viz., 3.5NiCrMoV and CrMoV turbine rotor steels and 2.25Cr-1Mo pressure vessel steel.[44] The purpose of this paper is to present the important effects of Mn, Si, and impurities which should control the design of these high-temperature bainitic alloy steels. Key results will be used to illustrate the influences of Mn, Si, and impurities on cleanliness, overheating, austenitizing, hardenability, tempering, ductility, toughness, temper embrittlement, creep rupture, and low-cycle fatigue. Examples illustrating the implementation of the results and the effectiveness of the alloy design guidelines are also provided.

II. EXPERIMENTAL PROCEDURES

A. Preparation of the Steels

The compositions of the 3.5NiCrMoV, CrMoV, and 2.25Cr-1Mo steels that were studied are compared to the appropriate ASTM specifications in Table I. The J factor for each of the steels is also included in Table I. The commercial-purity steels, designated CP (J factors of 31 to 131), were prepared and studied by Bethlehem Steel Corporation, Bethlehem, PA; they typify standard electric arc furnace steel. The high-purity steels, designated HP (J factors of 2 to 8), were prepared and studied by Japan Steel Works, Ltd., Muroran, Japan. Manganese

Table I. Compositions of the Steels in Weight Percent

Grade	Steel	C	Mn	Si	P	S	Ni	Cr	Mo	V	Cu	Al	Sn	As	Sb*	N*	O*	J**
3.5NiCrMoV	HP	0.24	0.03	0.03	0.003	<0.001	3.55	1.79	0.44	0.11	0.01	<0.004	<0.002	<0.001	9	8	13	2
	HP + 0.2Mn	0.25	0.19	0.02	0.003	0.001	3.57	1.78	0.44	0.10	0.01	<0.004	<0.002	<0.001	7	9	17	8
	HP + Sn + As + Sb	0.25	0.03	0.03	0.004	<0.001	3.61	1.76	0.44	0.11	0.01	<0.004	0.011	0.006	12	8	18	9
	CP + 0.2Mn	0.24	0.17	0.01	0.010	0.008	3.57	1.68	0.44	0.10	0.01	0.006	0.010	0.006	16	18	13	36
	CP + 0.35Mn	0.24	0.37	0.01	0.010	0.008	3.52	1.67	0.44	0.10	0.01	0.005	0.010	0.006	14	18	14	76
	A470-Cl. 7	≦0.28	$\frac{0.20}{0.60}$	≦0.10	≦0.015	≦0.018	$\frac{3.25}{4.00}$	$\frac{1.25}{2.00}$	$\frac{0.25}{0.60}$	$\frac{0.05}{0.15}$								
CrMoV	HP	0.29	0.02	0.03	0.002	<0.001	0.36	1.16	1.17	0.25	0.01	<0.004	<0.002	<0.001	9	10	17	2
	HP Comp.	0.29	0.02	0.04	0.002	0.001	0.91	1.60	1.37	0.25	0.01	<0.004	<0.002	<0.001	7	12	19	2
	HP + 0.2Mn	0.28	0.24	0.02	0.002	<0.001	0.38	1.17	1.19	0.25	0.01	<0.004	<0.002	<0.001	<5	9	14	8
	HP + 0.2Si	0.29	0.03	0.23	0.002	<0.001	0.36	1.18	1.16	0.25	0.01	0.005	<0.002	<0.001	7	8	14	8
	CP + 0.2Si	0.29	0.74	0.20	0.006	0.005	0.36	1.14	1.18	0.24	0.01	0.006	0.008	0.006	13	15	16	132
	CP + 0.2Mn	0.29	0.21	0.01	0.006	0.006	0.36	1.14	1.18	0.24	0.01	0.005	0.008	0.006	14	23	14	30
	CP + 0.75Mn	0.28	0.77	0.01	0.005	0.006	0.36	1.13	1.19	0.24	0.01	0.006	0.008	0.006	14	14	15	101
	A470-Cl. 8	$\frac{0.25}{0.35}$	≦1.00	$\frac{0.15}{0.35}$	≦0.015	≦0.018	≦0.75	$\frac{0.90}{1.50}$	$\frac{1.00}{1.50}$	$\frac{0.20}{0.30}$								
2.25Cr-1Mo	HP	0.15	0.02	0.02	0.003	<0.001	0.21	2.20	0.95	0.01	0.01	<0.004	<0.002	<0.001	10	10	24	2
	HP + 0.2Mn	0.15	0.24	0.04	0.002	<0.001	0.21	2.29	0.98	0.01	0.01	<0.004	<0.002	<0.001	9	13	27	8
	HP + 0.2Si	0.15	0.03	0.23	0.002	<0.001	0.21	2.30	1.00	0.01	0.01	<0.004	<0.002	<0.001	12	23	19	8
	CP + 0.2Si	0.16	0.47	0.21	0.009	0.010	0.21	2.30	0.99	<0.01	0.01	0.004	0.009	0.007	14	19	23	122
	CP + 0.2Mn	0.14	0.21	0.01	0.010	0.011	0.21	2.31	0.99	<0.01	0.01	0.005	0.009	0.006	18	18	18	42
	CP + 0.45Mn	0.14	0.47	0.01	0.009	0:010	0.21	2.33	0.98	<0.01	0.01	0.004	0.010	0.006	20	20	19	91
	A336-F22	≦0.15	$\frac{0.30}{0.60}$	≦0.50	≦0.030	≦0.030		$\frac{2.00}{2.50}$	$\frac{0.90}{1.10}$									

*ppm
**J = (pct Mn + pct Si) × (pct P + pct Sn) × 10^4

was studied at conventional levels and at levels where the Mn/S ratio was approximately 20:1 or greater to avoid overheating with normal processing. Silicon was studied at nominal levels of 0.02 and 0.20 pct, typifying vacuum carbon deoxidation and silicon deoxidation practices, respectively. The nominal levels of the impurity elements in the CP and HP steels were 0.008 pct P, 0.008 pct S, 0.008 pct Sn, 0.006 pct As, and 0.0015 pct Sb, and 0.003 pct P, 0.001 pct S, 0.002 pct Sn, 0.001 pct As, and 0.0009 pct Sb, respectively. In the case of the 3.5NiCrMoV grade, an HP steel with commercial residual levels of Sn, As, and Sb (J factor of 9) was also investigated to determine its resistance to temper embrittlement.

The 18 steels were made in laboratory vacuum-induction furnaces using high-purity Showa Denko Atomiron XL electrolytic iron and high-purity alloying elements. The steels were cast as either 100 (HP) or 225 (CP) kg ingots and hammer forged to plates measuring 35 mm thick × 150 mm wide. Following forging, each of the plates was sectioned, normalized, and tempered using the times and temperatures listed in Table II. The preliminary heat-treatment temperatures were chosen to be consistent with the production practices employed for these different steels. The purposes of the preliminary heat treatment are (a) homogenization, (b) softening for machinability, (c) refinement of the as-forged microstructure, and (d) conditioning of the microstructure for further refinement during the final heat treatment.

Dilatometer pins measuring 2.5 mm in diameter × 50 mm long were machined from each steel in the normalized and tempered condition, and the critical temperatures upon heating (rate of 55 °C/h) were determined. Partial continuous-cooling-transformation (C-C-T) diagrams were also developed for each of the steels by austenitizing the dilatometer pins for 20 minutes and cooling at various rates. The austenitizing temperatures for the 3.5NiCrMoV, CrMoV, and 2.25Cr-1Mo steels were 840 °C, 950 °C, and 900 °C, respectively. Linear regression analyses were performed to establish the influence of the alloying elements on the critical transformation temperatures during cooling.

The aim experimental control parameters for each of the grades are summarized in Table III. Each particular grade of steel was cooled from the austenitizing temperature at an average rate which simulates the center of a typical full-size component. The corresponding average center cooling rates, component thicknesses, and quenching media are included in Table III. The partial C-C-T diagrams were used to verify and/or establish a faster cooling rate than those listed in Table III, which would result in a fully bainitic microstructure.* The aus-

---

*As will be shown later, this was not done in the case of the HP CrMoV steels.

---

tenite grain size was controlled by varying time at the austenitizing temperature. Tensile strength was controlled by varying time at the tempering temperature. The resultant final heat-treatment cycles are summarized in Table IV. The 2.25Cr-1Mo steels were tempered at 650 °C and subsequently given a simulated stress relief treatment at 680 °C for either 20 (HP) or 28 (CP) hours. Although most of the mechanical properties were developed for the heat-treatment conditions shown in Table IV, selected tests were also conducted on material which was (a) water quenched from the final tempering temperature, (b) step cooled from the final tempering temperature, and (c) isothermally aged at 480 °C for 10,000 hours subsequent to the tempering heat treatments. To assess their resistance to temper embrittlement, the 3.5NiCrMoV and 2.25Cr-1Mo steels were step cooled according to the cycle of Gould:[3] furnace cool from the tempering temperature to 540 °C, hold 15 hours; furnace cool to 525 °C, hold 24 hours; furnace cool to 495 °C, hold 48 hours; furnace cool to 470 °C, hold 72 hours; and furnace cool to below 315 °C, remove from furnace, and air cool.

The CrMoV steels, which are known to be more resistant to temper embrittlement, were step cooled according to the more severe embrittlement cycle of Swaminathan et al.:[41] furnace cool from the tempering temperature to 540 °C, hold 15 hours; furnace cool to 510 °C, hold 15 hours; furnace cool to 480 °C, hold 24 hours; furnace cool to 470 °C, hold 72 hours; furnace cool to 430 °C, hold 100 hours; furnace cool to 400 °C, hold 168 hours; and furnace cool to room temperature.

To assess their susceptibility to overheating, selected steels were heated to temperatures between 1100 °C and 1400 °C for one hour, cooled at a rate of 2 °C/min to 900 °C, and then oil quenched. Following the initial austenitizing treatment, all of the steels were reaustenitized for one hour, oil quenched, tempered for one hour, and water quenched using the respective austenitizing and tempering temperatures listed in Table IV. Further experimental details on this work are described by Hale et al.[45]

Table II. Preliminary Heat Treatments

| Grade | Type* | Normalizing | | Temper | |
		Temp. (°C)	Time (h)	Temp. (°C)	Time (h)
3.5NiCrMoV	HP	940	3	650	5
	CP	940	6	650	10
CrMoV	HP	1020	3	680	5
	CP	1020	6	680	10
2.25Cr-1Mo	HP	920	3	650	5
	CP	920	6	650	10

*HP and CP stand for high-purity and commercial-purity, respectively.

Table III. Aim Experimental Control Parameters

Grade	Average Cooling Rate from Austenitizing Temperature (°C/min)	Center Cooling Rate Equivalent (mm)	Austenite Grain Size		Tensile Strength (MPa)
			(μm)	ASTM No.	
3.5NiCrMoV	1.1	1780, water spray quenched	20 to 40	8 to 6	870
CrMoV	0.8	1270, fan air quenched	30 to 60	7 to 5	765
2.25Cr-1Mo	14	305, water quenched	30 to 60	7 to 5	540

Extensive light microscopy was performed throughout the study. Longitudinal samples were examined using a Leitz image analysis system. Inclusions were characterized by examining at least 100 fields and 100 inclusion particles per sample in the unetched condition. The elemental components of selected inclusions were identified with the use of an ARL EMXSM electron microprobe. Polished and etched specimens were also examined for general microstructure. Various etchants were used to delineate microstructures for the different grades of steel. The volume fractions of ferrite, pearlite, and bainite in the microstructure were established through point counting. Prior-austenite grain size was measured by the three-circle intercept method of ASTM E112. Carbon extraction replicas were also prepared in selected cases and examined in a PHILIPS EM300* transmission elec-

---

*PHILIPS EM300 is a trademark of Philips Instruments.

---

tron microscope and a VG Scientific model HB501 dedicated scanning transmission electron microscope, both of which were operated at 100 kV. The VG microscope was equipped with a computer-based energy dispersive spectrometer (EDS) X-ray analyzer for identifying elements present in the precipitates. Selected fracture faces were examined in an Amray scanning electron microscope.

B. Mechanical Property Testing

All of the test specimens employed were tested transverse to the primary deformation direction. For the Charpy and fracture toughness tests, the notch was machined in the standard "T-L" orientation as described in ASTM E399.

Both Rockwell "C" and diamond pyramid (10 kg load)

hardness tests were conducted on the tempering series and dilatometer specimens, respectively. Duplicate tensile tests were performed between room temperature and 550 °C using standard ASTM 12.8-mm-diameter specimens. Twelve standard size ASTM Charpy V-notch specimens were used to establish a 50 pct FATT. Duplicate tests were conducted in the upper-shelf regime to establish the upper-shelf energy. Charpy specimens from the overheating series were also broken in the upper shelf regime to assess the susceptibility of the steels to overheating.

The J integral fracture toughness tests were performed in accordance with ASTM E813, using 1T compact tension specimens to estimate the nonlinear toughness, J_{Ic}. Tests were conducted in air between room temperature and 540 °C. The J_{Ic} was estimated for each steel where possible through a J-R curve developed using the single-specimen unloading compliance method. The J_{Ic} was converted to K_{Ic} through the following relationship:

$$K_{Ic} = \sqrt{(J_{Ic} \times E)/(1 - \nu^2)} \qquad [2]$$

where ν and E are Poisson's ratio (0.3) and Young's modulus, respectively. Standard Westinghouse combination notch-smooth bar specimens with a diameter of 9.1 mm were used for the creep rupture testing. Tests were conducted at 565 °C for the CrMoV and 2.25Cr-1Mo steels and 500 °C for the 3.5NiCrMoV steels.

Strain-controlled fatigue tests were performed on hourglass specimens with a minimum diameter of 7 mm. All tests were performed according to ASTM E606 at room temperature in air. The wave form was triangular, and the test frequency was altered between 1/30 and 1/3 Hz, depending on the strain amplitude. Strain amplitudes were selected so that the resulting lives were on the order of 10^3 to 10^4 cycles.

Table IV. Final Heat Treatments

Grade	Type*	Austenitizing		Quench Rate (°C/min)	Tempering Temp. (°C)	Cooling Rate from Final Temper (°C/h)
		Temp. (°C)	Time (h)			
3.5NiCrMoV	HP	840	8	1.1	590	10
	CP	840	10	1.1	590	30
CrMoV	HP	950	2	0.8	680	10
	CP1	950	10	0.8	680	10
	CP2	950	10	3.3	680	85
2.25Cr-1Mo	HP	900	3	14	650/680	10
	CP	900	10	32	650/680	15

*HP and CP stand for high-purity and commercial-purity, respectively.

III. RESULTS AND DISCUSSION

Table V summarizes the microstructure, tensile strength, and critical temperatures for each of the steels. From this table, it is evident that the aim austenite grain sizes and tensile strengths were generally achieved. The tensile strengths for the 3.5NiCrMoV and CrMoV steels were controlled to within ±24 MPa. The 2.25Cr-1Mo steels exhibited greater variation (±40 MPa) in tensile strength due to the simulated stress relief heat treatments employed subsequent to the tempering heat treatment. Each of the steels consisted of a fully bainitic microstructure with the exception of the CrMoV steels, which were cooled at a rate of 0.8 °C/min and contained as much as 67 pct ferrite. With a cooling rate of 3.3 °C/min, all of the CrMoV steels were fully bainitic. Representative photomicrographs of the three grades are presented in Figure 2. The Ac_3 temperatures in Table V indicate that each of the steels was fully austenitic at the aim austenitizing temperatures. The Ac_1 temperatures in Table V indicate that each of the steels was tempered below the intercritical regime, i.e., ferrite and austenite. Having established the experimental controls for our investigation, we will now present selected key results to illustrate the influences of Mn, Si, and impurities on cleanliness, overheating, austenitizing, hardenability, tempering, ductility, toughness, temper embrittlement, creep rupture, and low-cycle fatigue.

A. Cleanliness

In general, the CP steel contained primarily MnS and complex aluminate-type inclusions based on electron microprobe analysis. These inclusions were found to occur separately, as well as in combinations. On the other hand,

the HP steels contained mostly complex aluminate-type inclusions with no evidence of MnS inclusions, thus indicating that the MnS inclusions were either in solution or unresolvable. Both the HP and CP steels with 0.20 pct Si contained some complex silicate-type inclusions. Quantitative microcleanliness results are presented in Table VI. As expected, the HP steels contain a lower total volume percentage of inclusions compared to the CP steels, presumably due to the absence of MnS-type inclusions. While Si content did not significantly influence the inclusion volume percentage, Mn content did affect the inclusion volume fraction in both the HP and CP steels. That is, for similar S and O levels, the steels containing less Mn were found to be cleaner. The reason for the improvement in cleanliness in the HP steel when the Mn content is lowered is unclear. However, the improvement in cleanliness in the CP steel when Mn content is lowered is attributed to a reduction in the volume fraction of MnS inclusions. As shown in Figure 3, the total inclusion content of these steels is related to the product of Mn and S contents.

Solubility isotherms for MnS in austenite for a series of temperatures between 900 °C and 1250 °C are given in Figure 4 (calculated from the solubility product of Turkdogan et al.[46]). Compositions to the right of (or above) a given boundary lie within the two-phase field; hence, some MnS will be present at that temperature. The Mn and S ranges for the CP and HP steels are also outlined in this figure. It is evident that some or all of the MnS inclusions in the HP steels (0.02 pct Mn and 0.001 pct S) are dissolved during the austenitizing treatment (depending on temperature). In this case, some of the dissolved MnS may reprecipitate upon cooling from the austenitizing temperature. Since the HP + 0.2Mn and the CP steels lie within the two-phase field, most of

Table V. Summary of Microstructure, Tensile Strength, and Critical Temperatures

| Grade	Steel	Quench Rate (°C/min)	Austenite Grain Size μm	Austenite Grain Size ASTM No.	Pct Ferrite	Pct Bainite	Tensile Strength (MPa)	Ac_1 (°C)	Ac_3 (°C)	Bs (°C)
3.5NiCrMoV	HP	1.1	21	7.8	0	100	862	740	806	502
	HP + 0.2Mn	1.1	25	7.3	0	100	862	720	778	480
	HP + Sn + As + Sb	1.1	21	7.8	0	100	891	730	796	489
	CP + 0.2Mn	1.1	23	7.5	0	100	890	722	797	522
	CP + 0.35Mn	1.1	27	7.1	0	100	845	713	800	485
CrMoV	HP	0.8	36	6.3	34	68	768	769	882	—
	HP Comp.	0.8	38	6.1	0	100	754	783	862	532
	HP + 0.2Mn	0.8	43	5.8	48	52	741	774	854	—
	HP + 0.2Si	0.8	62	4.7	62	38	765	779	867	—
	CP + 0.2Si	0.8	60	4.8	9	91	786	760	854	532
	CP + 0.2Si	3.3	60	4.8	0	100	762	—	—	—
	CP + 0.2Mn	0.8	31	6.7	67	33	767	764	864	560
	CP + 0.2Mn	3.3	31	6.7	0	100	790	—	—	—
	CP + 0.75Mn	0.8	58	4.9	3	97	778	757	852	532
	CP + 0.75Mn	3.3	58	4.9	0	100	772	—	—	—
2.25Cr-1Mo	HP	14	50	5.3	0	100	555	805	892	577
	HP + 0.2Mn	14	50	5.3	0	100	562	793	884	569
	HP + 0.2Si	14	44	5.7	0	100	582	793	882	—
	CP + 0.2Si	32	36	5.3	0	100	555	790	877	540
	CP + 0.2Mn	32	33	6.5	0	100	522	796	882	552
	CP + 0.45Mn	32	45	5.6	0	100	502	788	869	540
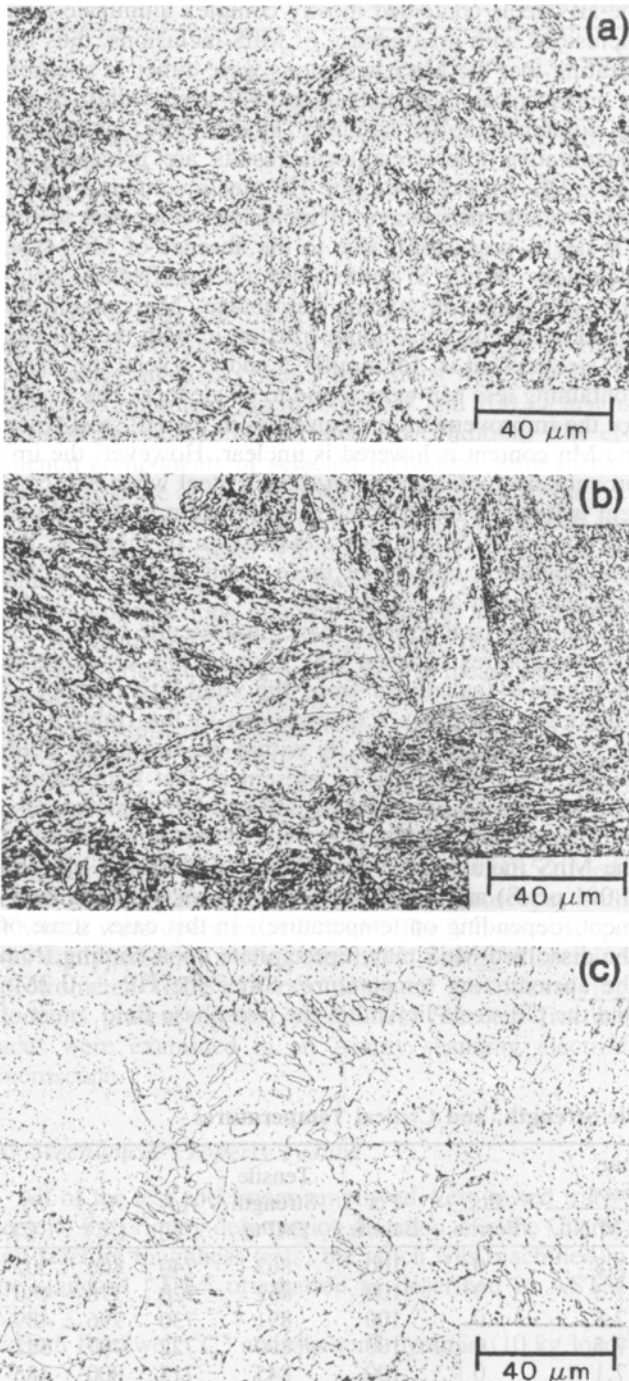
Fig. 2—Representative light micrographs illustrating the simulated quenched and tempered bainitic microstructures in the (a) CP + 0.35Mn 3.5NiCrMoV (nital), (b) CP + 0.2Si CrMoV (saturated picric + HCl), and (c) CP + 0.2Si 2.25Cr-1Mo (picral + HCl) steels.

Table VI. Quantitative Microcleanliness Results

Grade	Steel	Total* Vol Pct
3.5NiCrMoV	HP	0.007 ± 0.004
	HP + 0.2Mn	0.015 ± 0.009
	HP + Sn + As + Sb	0.006 ± 0.002
	CP + 0.2Mn	0.017 ± 0.006
	CP + 0.35Mn	0.027 ± 0.012
CrMoV	HP	0.005 ± 0.002
	HP Comp.	0.006 ± 0.003
	HP + 0.2Mn	0.010 ± 0.003
	HP + 0.2Si	0.006 ± 0.001
	CP + 0.2Si	0.022 ± 0.008
	CP + 0.2Mn	0.016 ± 0.005
	CP + 0.75Mn	0.028 ± 0.010
2.25Cr-1Mo	HP	0.012 ± 0.004
	HP + 0.2Mn	0.009 ± 0.003
	HP + 0.2Si	0.009 ± 0.004
	CP + 0.2Si	0.028 ± 0.015
	CP + 0.2Mn	0.014 ± 0.006
	CP + 0.45Mn	0.036 ± 0.015

*95 pct confidence limits

ancy between the CP steels as follows, using the CP 3.5 NiCrMoV steels, viz., the CP + 0.2Mn and CP + 0.35Mn steels, as an example. The Mn and S levels for these steels are plotted in Figure 4. Lines are shown parallel to the stoichiometric line for MnS from the respective compositional points to the 1250 °C phase boundary. These lines indicate that at a forging temperature of 1250 °C, 0.005 and 0.003 pct S are in solution for the

the sulfur in these steels is predicted to be out of solution and combined with Mn during the austenitizing treatments. This explains the greater volume percentage of inclusions (presumably, MnS inclusions which were too small to confirm using the electron microprobe) in the HP + 0.2Mn steels compared to the HP steels (Table VI).

At first glance, Figure 4 would predict similar volume fractions of MnS inclusions for the CP + 0.2Mn and the higher Mn CP steels. We have rationalized this discrep-

Fig. 3—Influence of the product of Mn and S on total inclusion content.

CP + 0.2Mn and CP + 0.35Mn steels, respectively. Upon cooling from the forging temperature and during subsequent heat treatments, much of the sulfur in solution is expected to reprecipitate as fine MnS particles. We speculate that perhaps these fine MnS particles were unresolvable in the light microscope. Hence, the improved cleanliness of the CP + 0.2Mn steel could be explained based on its larger volume fraction of fine, unresolvable MnS particles (or smaller volume fraction of MnS particles undissolved at the forging reheat temperature).

In summary, cleanliness was found to improve as both Mn and S levels were reduced. The unexpected Mn effect has been rationalized in terms of the solubility of MnS in austenite.

B. Overheating

Overheating is generally considered to involve the dissolution of some or all of the Mn-rich sulfides present in the steel at the reheating temperature (during hot working or austenitizing) and their subsequent reprecipitation along the austenitic boundaries during cooling. The presence of these Mn-rich sulfides along the austenitic grain boundaries can severely degrade the toughness of steel. Hale and Nutting[47] have reviewed the phenomenon of overheating in detail, covering its mechanisms, effects on mechanical properties, and some methods for its prevention through careful processing.

The upper shelf Charpy impact energy values for the 3.5NiCrMoV, 2.25Cr-1Mo, and CrMoV steels in the fully heat-treated condition after exposure to high temperatures are presented in Figure 5. Although there is variation in toughness among the steels shown due to the differences in microcleanliness, the HP and HP + 0.2Mn steels did not exhibit a decrease in impact energy as

Manganese, wt. %

Fig. 4 — Solubility isotherms for MnS in austenite for a series of temperatures between 900 °C and 1250 °C (calculated from the solubility product of Turkdogan et al.[46]). Typical Mn and S ranges for the HP and CP steels are indicated by shading. The two lines drawn parallel to the stoichiometric line are used to illustrate the amount of sulfur out of solution for the CP + 0.2Mn and CP + 0.35Mn 3.5NiCrMoV steels at 1250 °C.

(a)

(b)

(c)
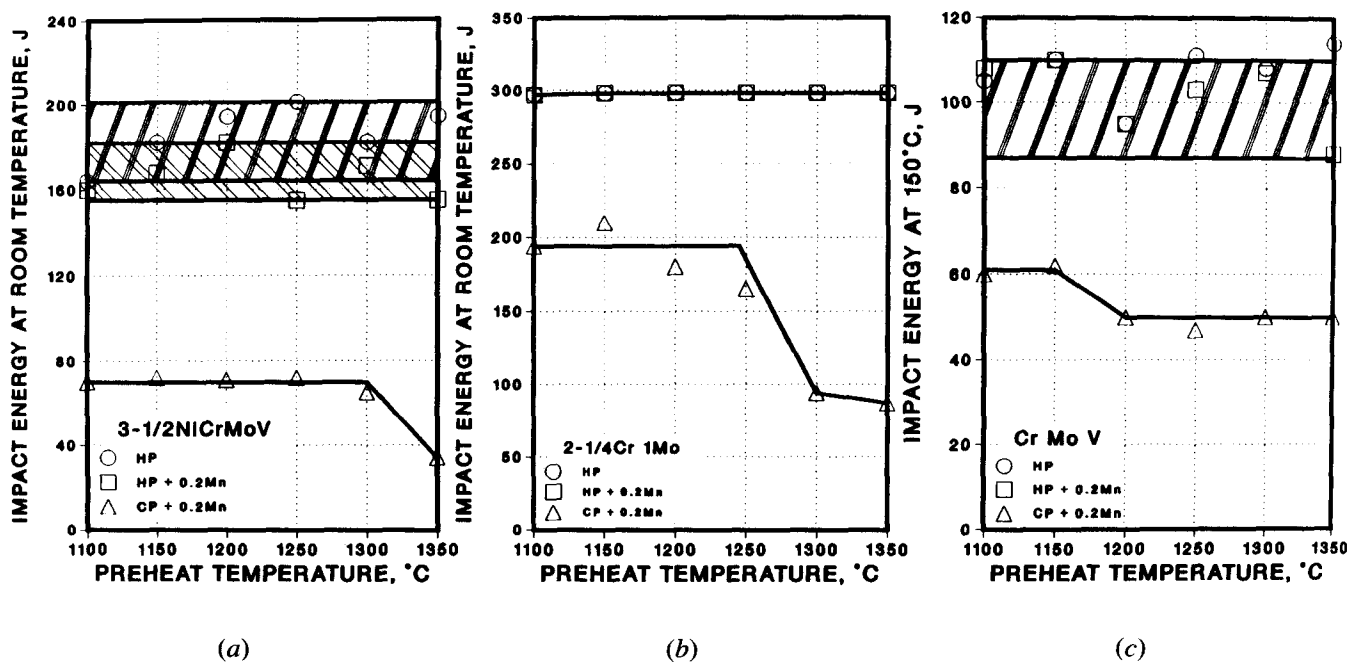
Fig. 5 — Influence of preheat temperature on the upper shelf Charpy impact energy for the (a) 3.5NiCrMoV, (b) 2.25Cr-1Mo, and (c) CrMoV steels which are in the austenitized, oil-quenched, and tempered conditions.

preheat temperature increased. On the other hand, the CP + 0.2Mn steels did exhibit a decrease in upper-shelf toughness for a particular preheat temperature, thus indicating that these steels are susceptible to overheating. This effect of overheating is well known and is the reason why, for example, the CP 3.5NiCrMoV steels are normally hot worked below 1250 °C. However, since the HP and HP + 0.2Mn steels are immune to overheating, at least up to 1400 °C, these steels could be hot worked at higher temperatures, thus requiring lower deformation loads (e.g., a smaller forging press could be utilized) and possibly fewer reheats (e.g., as in the forging of turbine rotors).

C. Austenitizing

To enhance both strength and toughness, a fine prior-austenite grain size in bainitic alloy steels is generally desired. As a result, the austenitizing temperature is normally maintained slightly above the Ac_3 temperature, e.g., Ac_3 + 45 °C.[48] For these steels, the Ac_3 temperature was found to be related to Mn, Ni, and Cr by the following equation (the multiple coefficient of determination, R^2 = 0.96):

$$Ac_3(°C) = 868 - 27(\text{pct Mn})$$
$$- 24(\text{pct Ni}) + 10(\text{pct Cr}) \qquad [3]$$

This equation is different from that of Andrews[49] in that it contains Mn and Cr. From Eq. [3], it is evident that the Ac_3 temperature decreases with increasing Mn content, while variations in Si over the range of 0.02 to 0.20 pct do not have a significant effect on Ac_3. Hence, if Mn is removed from the steel to improve temper embrittlement resistance, the austenitizing temperature may need to be increased accordingly.

Figure 6(a) shows the effect of austenitizing time at 900 °C on the average austenite grain size of the 2.25Cr-1Mo steels. In this grade, which contains no micro-alloying elements for austenite grain refinement, the HP steels coarsen at a more rapid rate compared to the CP steels, thus suggesting that inclusion content does contribute to austenite grain refinement. Interestingly, the austenite grain size of the CP + 0.2Mn steel is always finer than the CP + 0.45Mn steel for a given austenitizing time. This effect is presumably due to the finer (unresolvable) MnS inclusions in the CP + 0.2Mn steel (as discussed previously), which are more effective in pinning austenite grain boundaries. This effect has also been noted previously by Abiko et al.[50] for 2.25Cr-1Mo steels. Conversely, in a 3.5NiCrMo steel which has been microalloyed with 0.10 pct V (i.e., 3.5NiCrMoV), the austenite grain sizes of both the HP and CP steels coarsen at a similar rate, as illustrated in Figure 6(b). This is attributed to the presence of fine carbonitrides which can pin austenite grain boundaries. A photomicrograph displaying these carbonitrides (12 to 24 nm in diameter) along a prior-austenite grain boundary in the HP 3.5NiCrMoV steel, which has been austenitized at 840 °C for eight hours and cooled at a rate of 1.1 °C/min to room temperature, is presented in Figure 7(a). Through X-ray microanalysis, these particles were determined to
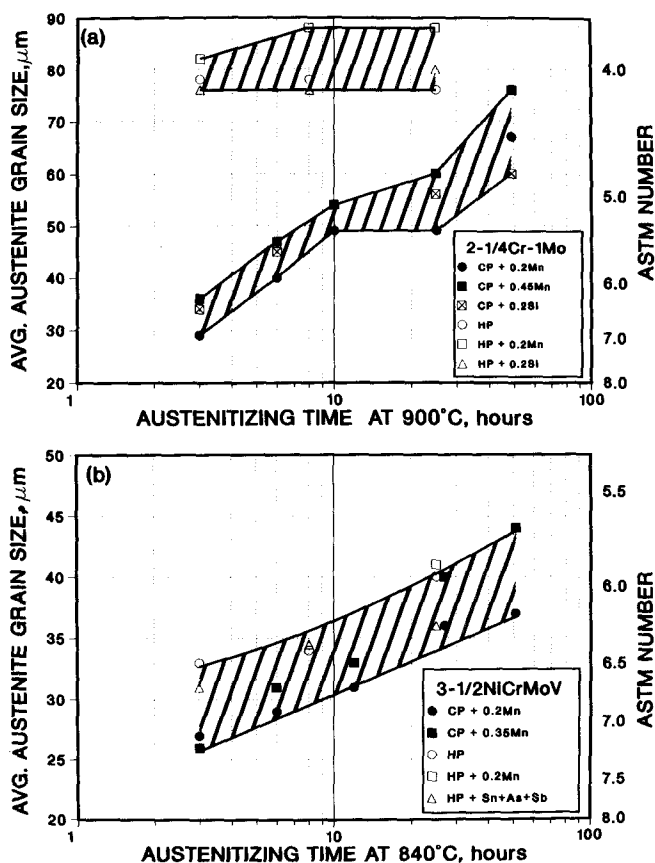

Fig. 6—Influence of austenitizing time on the average austenite grain size of the (a) 2.25Cr-1Mo and (b) 3.5NiCrMoV steels.

be rich in Mo, V, and Cr, as shown in Figure 7(b). The C, O, and Si peaks are from the carbon replica, and the Cu peak is from the copper support grid.

D. Hardenability

The hardenability of bainitic steels is usually discussed in terms of the position of the ferrite nose on a C-C-T diagram. The effects of Mn and Si in the CrMoV steels on the partial C-C-T diagram, particularly the ferrite nose position and shape, are illustrated in Figure 8. Comparing Figures 8(a) and (b), it is evident that the hardenability is reduced as the Mn content is lowered, e.g., from 0.75 to 0.20 pct in the CP steels. On the other hand, comparing Figures 8(b) and (c), it is evident that the hardenability is increased when silicon is removed from the CP steel (e.g., at a cooling rate of 0.8 °C/min, there is 27 vs 37 pct ferrite). These diagrams make it clear why the lower-Mn and higher-Si CrMoV steels contained substantial amounts of free ferrite (Table V) after cooling at a simulated quench rate of 0.8 °C/min. Substantial amounts of free ferrite in the microstructure can result in a degradation in toughness. For example, the volume percentages of the microstructural constituents, tensile strength, and Charpy properties of the HP and CP + 0.75Mn steels are compared in Table VII. For similar tensile strengths (in the quenched and tempered condition), the 34 pct free ferrite in the HP steel raises
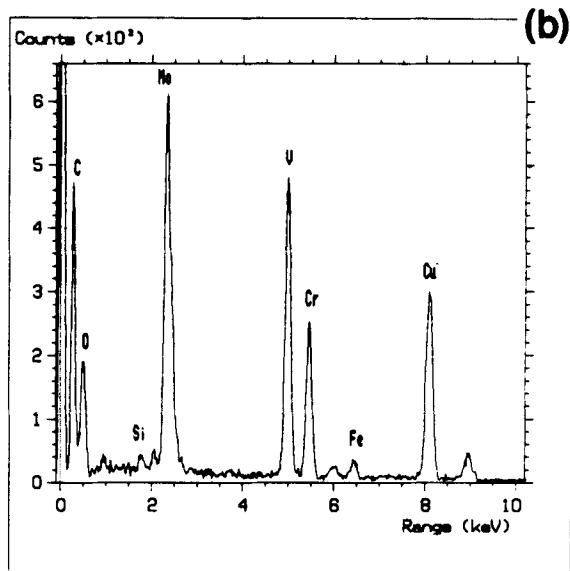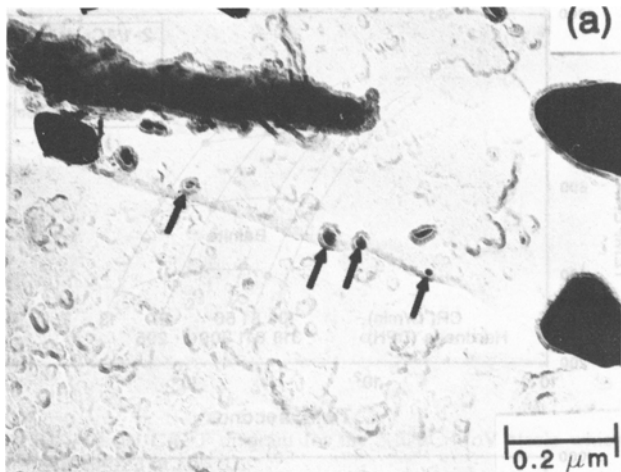
Fig. 7—Carbon extraction replica (a) illustrating fine carbonitrides (located by arrows) along a prior-austenite grain boundary in the HP 3.5NiCrMoV steel which has been austenitized and simulated quenched. The X-ray spectrum (b) provides evidence that these carbonitrides are rich in Mo, V, and Cr.

the 50 pct FATT by about 40 °C compared to the fully tempered bainitic CP + 0.75Mn steel.

Since the Bs temperature for a particular steel was found to be essentially constant for the range of cooling rates explored in this study, a regression equation for Bs
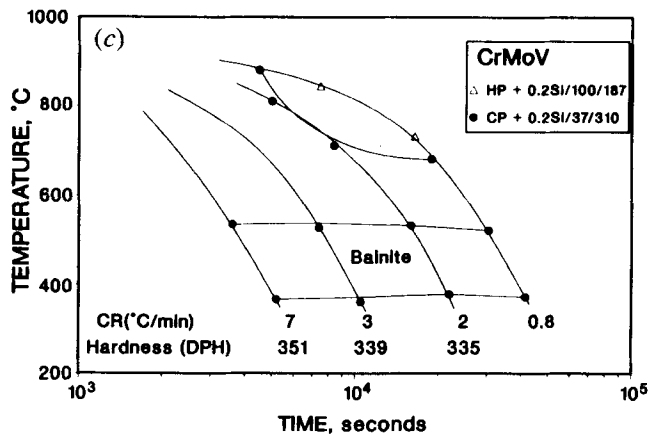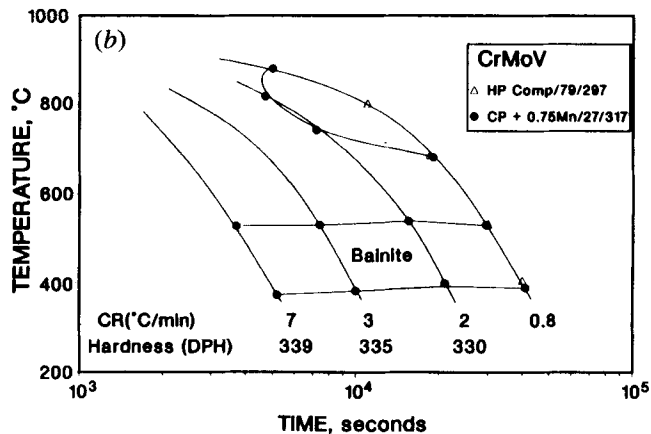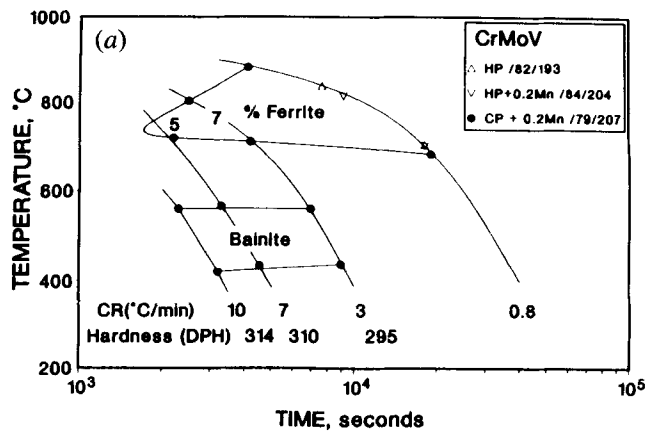
Fig. 8—Partial continuous C-C-T diagrams illustrating the influences of Mn and Si in a CrMoV steel on ferrite nose position and shape. The CrMoV steels were austenitized at 950 °C, and the legend designations are (a) steel, (b) percent ferrite, and (c) DPH hardness for a cooling rate of 0.8 °C/min.

Table VII.   Compensation for Loss in Hardenability for the CrMoV Steels

Steel	Pct Ferrite	Pct Bainite	Bs Temp. (°C)	Tensile Strength (MPa)	50 Pct FATT$_{WQ}$* (°C)	Upper Shelf Energy (J)
HP	34	66	—	768	129	113
CP + 0.75Mn	0	100	532	778	90	95
HP Comp.	0	100	532	754	77	138

*50 pct FATT upon water quenching from the tempering temperature.

temperature ($R^2 = 0.93$), utilizing the data in Table V, was established, viz.,

$$Bs(°C) = 844 - 597(pct\ C) - 63(pct\ Mn)$$
$$- 16(pct\ Ni) - 78(pct\ Cr) \qquad [4]$$

This equation is consistent with that of Steven and Haynes.[51] Since the elements that lower Bs temperature also increase hardenability, one can maintain the Bs temperature and compensate for the loss in hardenability due to a lower Mn content in the HP CrMoV steel by adding Ni and Cr, for example. In fact, this was our philosophy in designing the HP Comp. CrMoV steel (compensated with Ni, Cr, and Mo to maintain hardenability and Bs temperature). This steel was found to be fully bainitic and to have a Bs temperature identical to the CP + 0.75Mn steel, viz., 532 °C. Table VII also compares the Charpy impact toughness of the HP Comp. steel with the HP and CP + 0.75Mn steels. The HP Comp. steel not only exhibited better toughness than the HP steel but also displayed a higher level of toughness than the standard composition (i.e., CP + 0.75Mn).

The effects of Mn and Si on the ferrite nose position for the 2.25Cr-1Mo steels were found to be similar to the CrMoV steels,[52] as shown in Figure 9. However, essentially no loss in hardenability was noted when Mn was removed from the 3.5NiCrMoV steel for cooling rates as slow as 1.1 °C/min (Figure 10).

E. Tempering

The linear regression equation for Ac_1 temperature ($R^2 = 0.97$) is shown below.

$$Ac_1(°C) = 762 - 28(pct\ Mn)$$
$$- 18(pct\ Ni) + 19(pct\ Cr) \qquad [5]$$

This equation is consistent with that of Andrews.[49] From this equation, it is evident that Mn and Ni lower and Cr raises the Ac_1 temperature. The important point to note is that when the Mn content is lowered to improve temper embrittlement resistance and four times as much Ni is added to maintain a constant Bs temperature (Eq. [4]), the Ac_1 temperature may fall into the normal tempering range. Therefore, precautions may be required to avoid tempering in the intercritical regime.

The influence of tempering parameter on the hardness of the 3.5NiCrMoV, 2.25Cr-1Mo, and CrMoV steels is illustrated in Figures 11(a), (b), and (c), respectively. The 3.5NiCrMoV steels, which contain low levels of Si, all soften at a similar rate, as indicated by the band in Figure 11(a), whereas the 2.25Cr-1Mo steels, shown in Figure 11(b), soften at different rates. The Si-containing 2.25Cr-1Mo steels exhibit more temper resistance compared to the low-Si steels at similar Mn levels. This same effect of Si on temper resistance has been observed by others.[53] Barnard et al.[54] have confirmed the mechanism for the Si effect, which is as follows. Silicon is injected from growing cementite and forms an Si-rich .ferrite region around it. The Si-rich region makes it more difficult for carbon to diffuse to the growing cementite, since Si locally raises the activity of carbon and thus reduces the activity gradient. Therefore, tempering heat treatments may require adjustment when the Si content
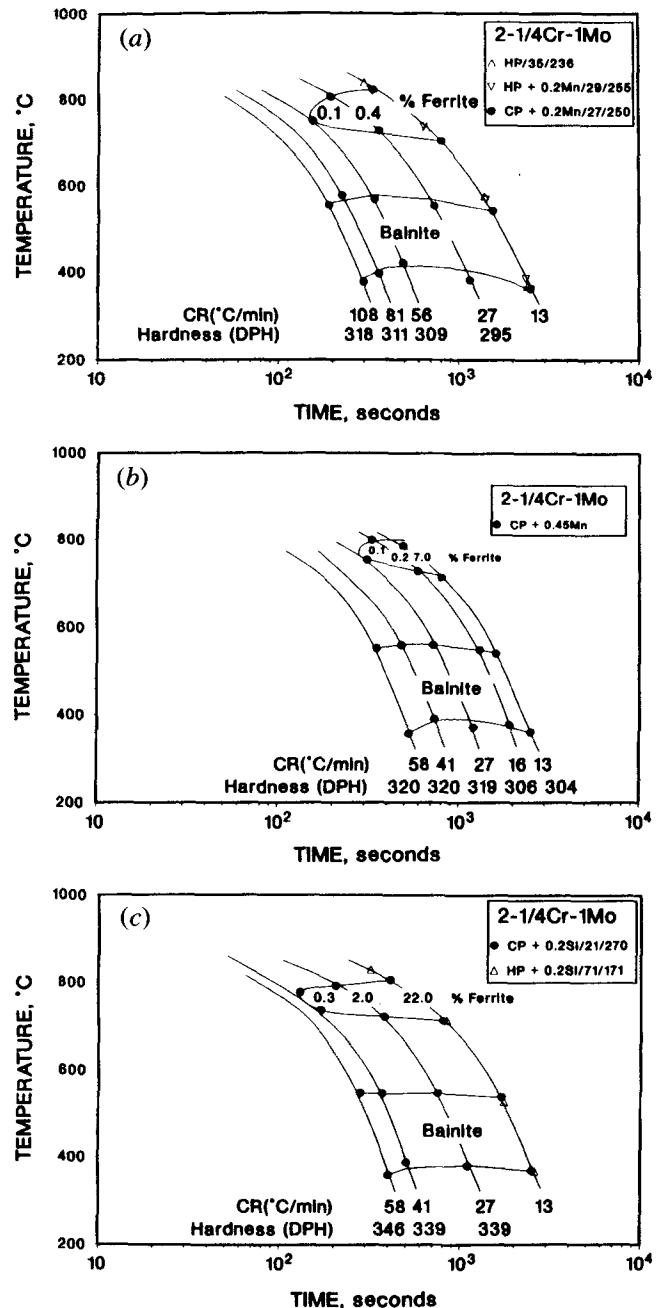

Fig. 9—Partial C-C-T diagrams illustrating the influences of Mn and Si in a 2.25Cr-1Mo steel on ferrite nose position and shape. The 2.25Cr-1Mo steels were austenitized at 900 °C, and the legend designations are (a) steel, (b) percent ferrite, and (c) DPH hardness for a cooling rate of 13 °C/min.

in bainitic steels is lowered, due to the possible loss in temper resistance.

Comparing the CP + 0.2Mn and CP + 0.45Mn 2.25Cr-1Mo steels, which were heat treated similarly, Mn does not appear to influence tempering resistance. However, if Mn is lowered to the HP level of 0.02 pct, the simulated as-quenched hardness may be reduced due to a higher Bs temperature (and, hence, a coarser bainitic microstructure). This is presumably the reason for the lower hardness of the HP steel in relation to the other steels in Figure 9(b) for a given tempering parameter. All of the tempered bainitic CrMoV steels exhibited a

Fig. 10—Partial C-C-T diagram for the 3.5NiCrMoV steels which were austenitized at 840 °C.

similar tempering response (Figure 11(c)). The impurity elements are not believed to significantly influence this tempering response.

F. Ductility

As expected, tensile ductility was found to be a function of inclusion content. For example, Figure 12 displays the influence of test temperature on tensile reduction of area for the 3.5NiCrMoV, 2.25Cr-1Mo, and CrMoV steels. This figure shows that the HP steels exhibit greater tensile ductility compared to the CP steels. Figure 12(a) shows that the CP + 0.2Mn steel exhibits slightly more ductility than the CP + 0.35Mn steel. This difference can be accounted for by the improved microcleanliness of the lower Mn steel. The minima in tensile ductility exhibited by most of the HP and CP steels are believed to be due to dynamic strain aging, as has been observed previously in other quenched and tempered bainitic steels, e.g., CrMoV.[55]

G. Toughness and Temper Embrittlement

Charpy 50 pct FATT, Charpy upper shelf energy, and K_{Ic} fracture toughness are all used to characterize the toughness of bainitic alloy steels. Figure 13 presents bar charts comparing these different measures of toughness in the 3.5NiCrMoV steels. In all three cases, the HP steels were found to be tougher than the CP steels. The higher toughness of the HP steels is not only attributed to their superior microcleanliness but also to their greater resistance to temper embrittlement. Upon examination of the lower-shelf Charpy fracture faces of the CP + 0.35Mn steel, some intergranular facets were observed (i.e., about 5 pct of the fracture surface), presumably due to temper embrittlement. This temper embrittlement is believed to be primarily related to the higher Mn and P levels in this particular steel, as has been observed previously in several other investigations.[20]

As discussed previously, temper embrittlement susceptibility is often assessed by measuring the shift in Charpy 50 pct FATT. Figure 14 compares the shifts in 50 pct FATT for step cooling and 10,000 hours of isothermal aging at 480 °C with a water-quenched condition for the 3.5NiCrMoV, 2.25Cr-1Mo, and CrMoV steels. Based on these data, we have confirmed what is well
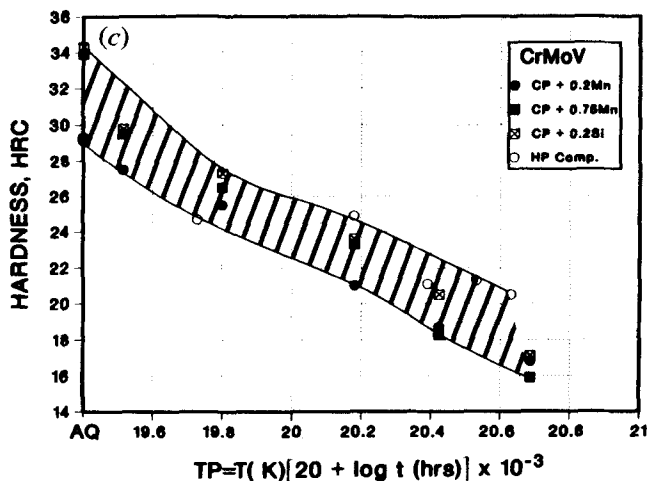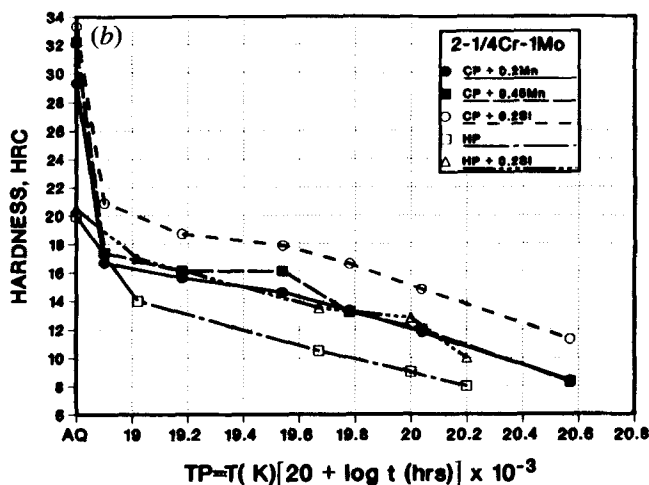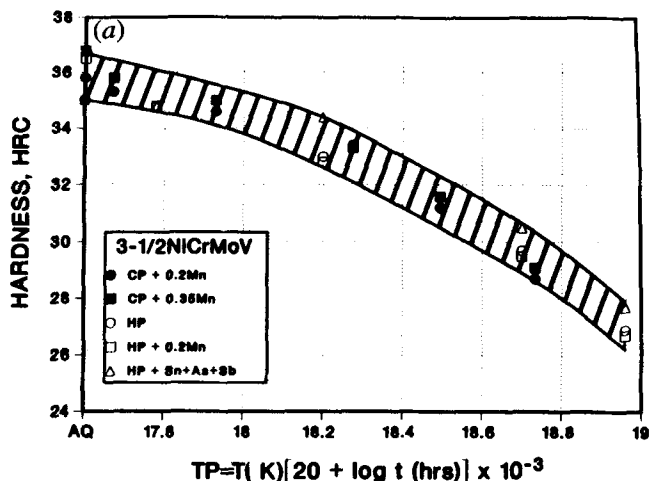
Fig. 11—Influence of tempering parameter (TP) on the hardness of the (a) 3.5NiCrMoV, (b) 2.25Cr-1Mo, and (c) CrMoV steels. AQ signifies the as-simulated quenched condition.

documented in the literature, i.e., that temper embrittlement can be correlated with the J factor. Specifically,

(1) the HP steels are essentially immune to temper embrittlement, with shifts in 50 pct FATT of <10 °C when aged at 480 °C for 10,000 hours;

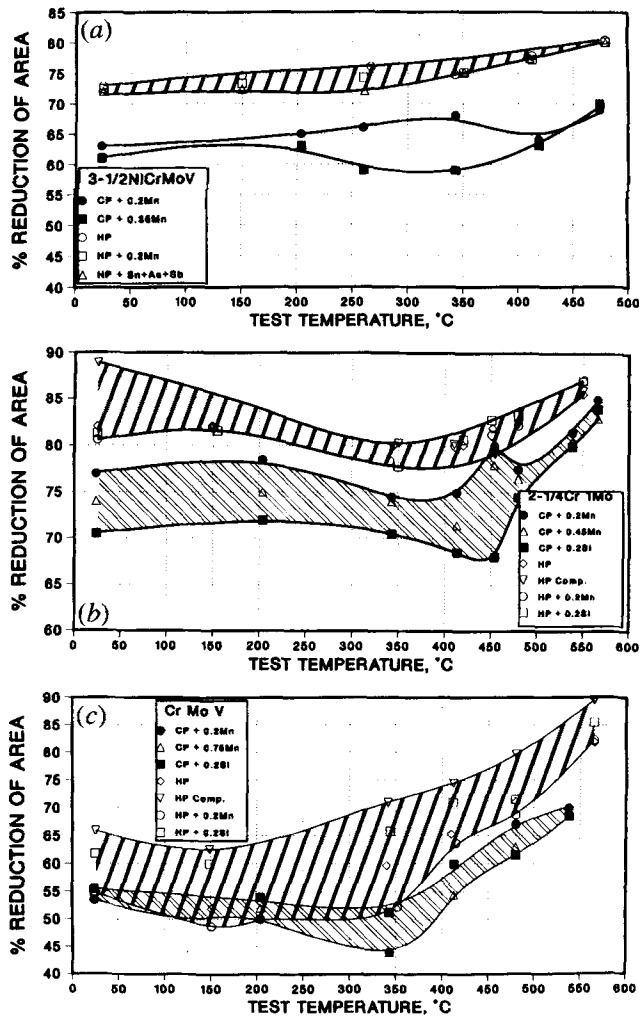(2) for the CP steels, a higher Mn and Si content makes

Fig. 12—Influence of test temperature on the tensile ductility of the
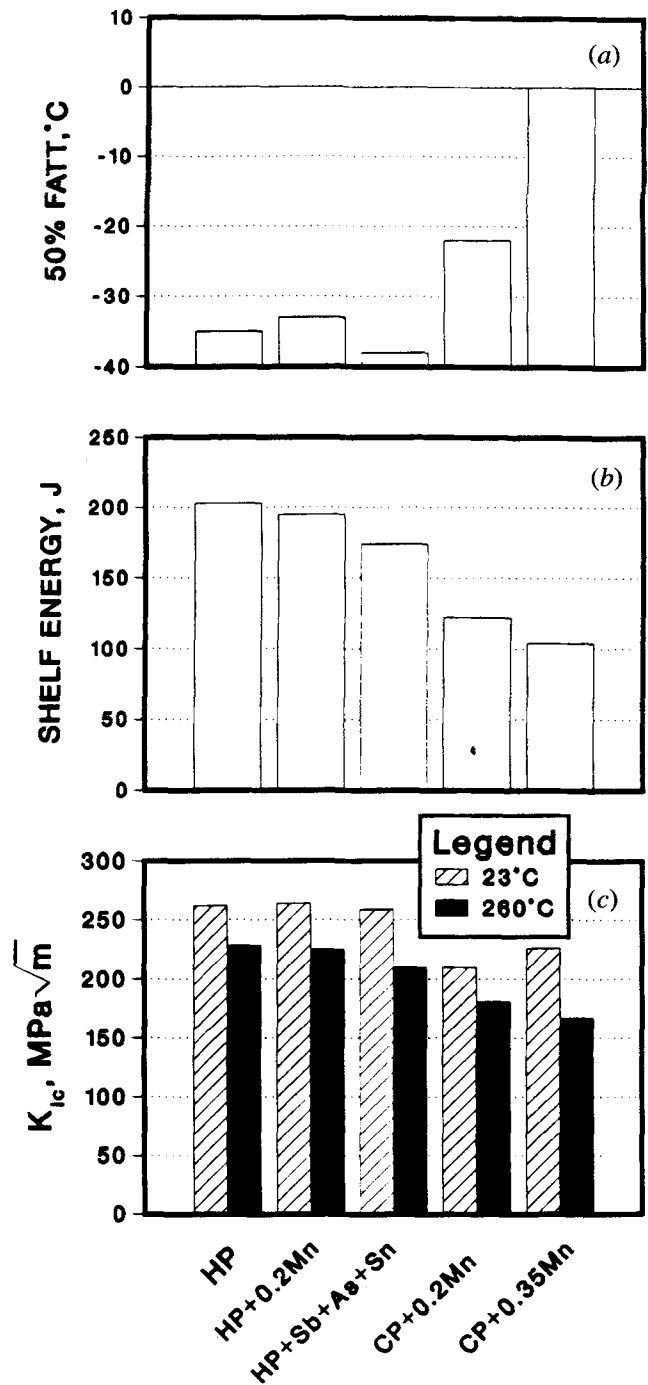(a) 3.5NiCrMoV, (b) 2.25Cr-1Mo, and (c) CrMoV steels.

Fig. 13—Bar charts illustrating the influence of compositional variations in the 3.5NiCrMoV steel on (a) Charpy 50 pct FATT, (b) Charpy upper shelf energy, and (c) fracture toughness, K_{Ic}.

these steels more susceptible to temper embrittlement;
and

(3) conventional levels of Sn + As + Sb in the HP steel
contribute to a slight degree of temper embrittlement (a
shift of about 20 °C in 50 pct FATT).

However, these elements are considered to be of secondary importance with regard to temper embrittlement
in comparison to the effects of Mn, Si, and P.

In summary, the HP steels were found to exhibit the
best toughness due to their high cleanliness level and
resistance to temper embrittlement.

H. Creep Rupture

Both Mn and Si were found to influence creep rupture
properties, while impurities did not, for tests of up to
10,000 hours. The creep rupture properties for the
3.5NiCrMoV, CrMoV, and 2.25Cr-1Mo steels are presented in Figures 15 through 17, respectively. From these
figures, it is evident that the lower-Mn HP steels exhibit
higher creep rupture strength compared to the higher-Mn
CP steels. This result is consistent with the subsequent
results of other researchers,[56,57,58] who found an improvement in creep rupture strength when the Mn content was lowered from 0.31 to 0.02 pct in a 3.5NiCrMoV
steel. The improvement in creep rupture strength in the
lower-Mn steel may be related to the presence of a greater
volume fraction of tempered upper bainite* in the micro-

*The volume fraction of upper bainite in these microstructures could
not be quantified.

structure, which has been shown by others[59,60] to contain a more uniform dispersion of fine, creep strength-controlling carbonitrides compared to a tempered lower
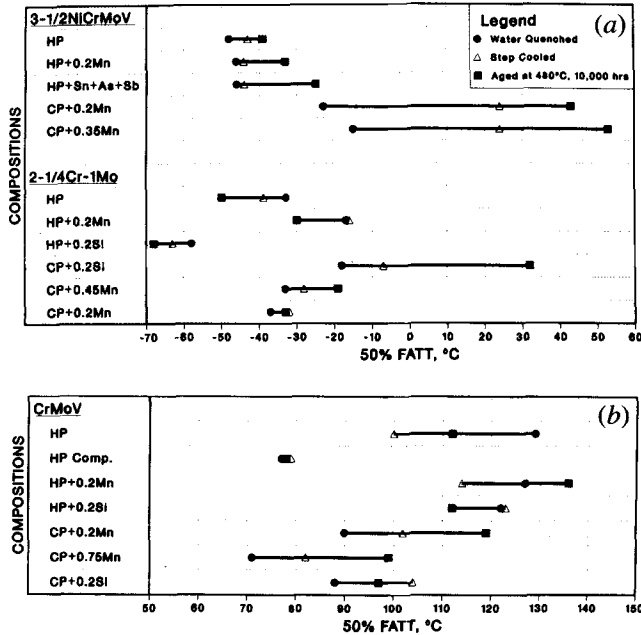bainitic steel. Several researchers[59,60,61] have observed

Fig. 14—Influences of step cooling and isothermal aging at 480 °C for 10,000 h on the shift of Charpy 50 pct FATT from the unembrittled water quenched from the tempering temperature condition for the (a) 3.5NiCrMoV and 2.25Cr-1Mo steels and (b) CrMoV steels.
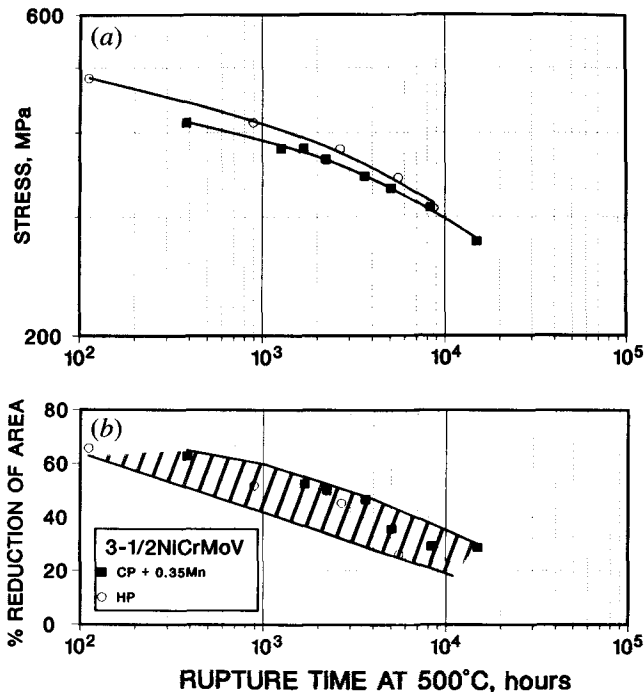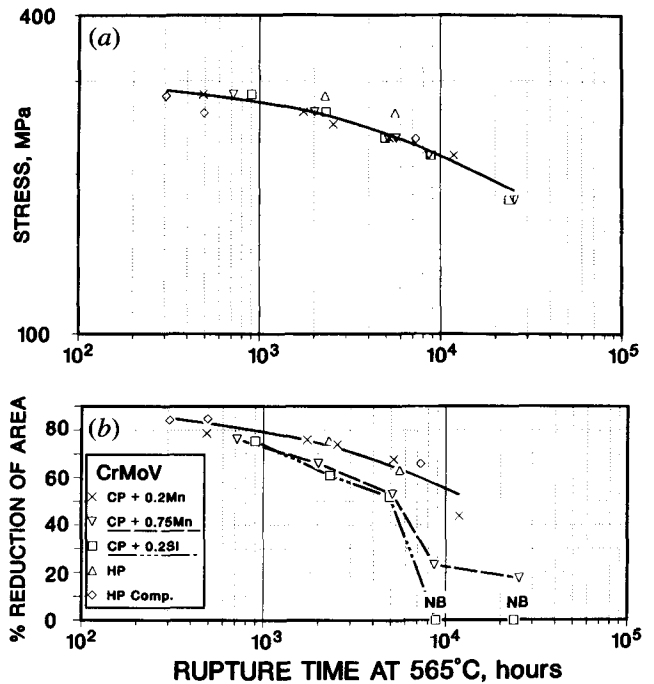
Fig. 16—Creep rupture (a) strength and (b) ductility plotted as a function of rupture time for the CrMoV steels which were tested at 565 °C. NB signifies that the specimen failed at the notch.

a superior balance of creep properties with tempered upper bainitic, as opposed to tempered lower bainitic, microstructures in CrMoV rotor steels.

Figure 15(b) shows that in the case of the 3.5NiCrMoV steels, the HP and CP + 0.35Mn steels exhibit similar creep rupture ductility. In the case of the CrMoV steels,

Figure 16(b) shows that the HP, HP Comp., and CP + 0.2Mn steels exhibit similar creep rupture ductility. Figure 16(b) also shows that the creep rupture ductility of the CrMoV steel improves as both Mn and Si contents are lowered. In addition to a greater percentage of upper bainite, the superior ductility of the HP and CP + 0.2Mn

Fig. 15—Creep rupture (a) strength and (b) ductility plotted as a function of rupture time for the HP and CP + 0.35Mn 3.5NiCrMoV steels which were tested at 500 °C.
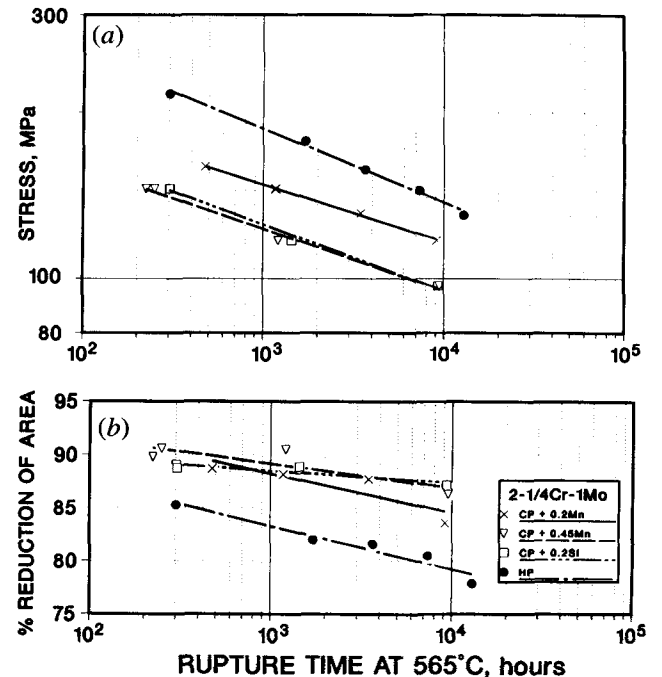
Fig. 17—Creep rupture (a) strength and (b) ductility plotted as a function of rupture time for the 2.25Cr-1Mo steels which were tested at 565 °C.

steels is also presumably due to their finer prior-austenite grain size in comparison with the other two CP steels (33 vs 59 μm). The CP + 0.75Mn steel exhibits improved creep rupture ductility compared to the CP + 0.2Si steel, clearly demonstrating the negative influence of Si on creep ductility. Room-temperature hardness testing after creep rupture resulted in similar levels in hardness in both steels, thus indicating that the improvement in creep ductility is not related to differences in strength. Swaminathan et al.[41] have also observed the superior creep ductility behavior in a low-Si CrMoV rotor steel, but the cause for the effect was not established.

In the case of the 2.25Cr-1Mo steels, the CP steels displayed similar rupture ductility to that of the HP steels, as shown in Figure 17(b). The slightly lower creep rupture ductility of the HP steel is presumably related to the trade-off in higher creep rupture strength.

I. Low-Cycle Fatigue

Neither Mn, Si, nor impurities were found to influence the low-cycle fatigue behavior of any of the steels. Data for all of the steels (Figure 18) support this point.

J. Stress Corrosion Cracking

In a related study, Magdowski and Speidel[62] have shown that the stress corrosion cracking rates of 3.5NiCrMoV steel in water exhibit no dependence on purity, compared with the HP, CP, and commercial varieties of this steel.

IV. IMPLEMENTATION OF RESULTS AND ALLOY DESIGN GUIDELINES

The following is a brief synopsis on how our conclusions and the resulting bainitic alloy steel design guidelines are being implemented.

A. 3.5NiCrMoV Steel

Based on advantages such as improved temper embrittlement resistance and creep rupture strength without any loss in hardenability or creep rupture ductility,
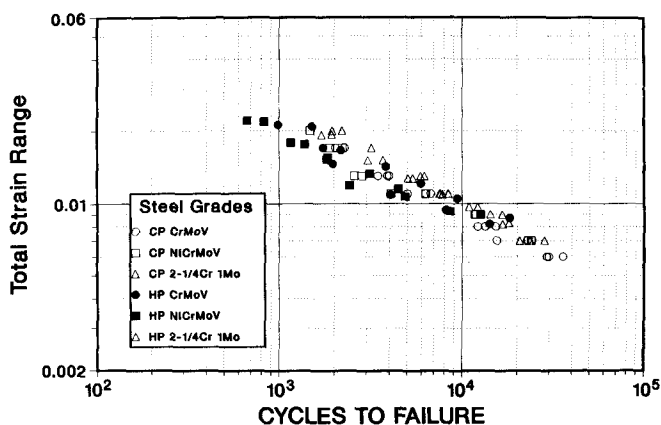

Fig. 18 — Room-temperature low-cycle fatigue data for all of the HP and CP steels.

several production ingots of high-purity 3.5NiCrMoV steel have been cast, forged, heat treated, and evaluated. These ingots have been forged into prototype rotors and studied by several forging producers and turbine builders, i.e., two 34-metric-ton ingots in Austria[63,64,65] and 105[66,67,68] and 50-metric-ton ingots in Japan.[69] Based on the positive results from these trials, Japan Steel Works, Ltd./Toshiba Corporation have produced four high-purity 3.5NiCrMoV turbine rotor forgings for two 700 MW Chubu Electric Kawagoe power plants in Japan. In addition, Japan Casting and Forging Corporation/Mitsubishi Heavy Industries have produced a 150 MW high-purity 3.5NiCrMoV steam turbine rotor for the Nagasaki Shipyard and Engine Works.[70]

Since the high-purity steel is essentially immune to temper embrittlement, lower tempering temperatures (within the temper embrittlement regime) are now permissible, thus allowing designers to take advantage of higher strength levels. Conversely, higher service temperatures (extending into the temper embrittlement regime) are permissible, since temper embrittlement is no longer a concern. The higher service temperatures can provide for improved efficiencies, e.g., elimination of the need for the cooling of steam before it enters a low-pressure turbine or rotor cooling. Laboratory work is continuing with the aim of further improving the creep rupture strength of this steel through the addition of nitrogen. Other applications under investigation for the new high-purity 3.5NiCrMoV steel include combination high-temperature–low-temperature property rotors, turbine discs, replacement of retired high-pressure NiMoV rotors, armor plate, guntubes and nuclear reactor, pressurizer, and steam generator pressure vessels.

B. CrMoV Steel

Laboratory work has continued with the goal of further improving the toughness of the HP Comp. steel. Improved toughness is required of CrMoV steam turbine rotors in order to eliminate the current need to prewarm the rotors above the 50 pct FATT before achieving full load. Prolonged startup and shutdown procedures require additional capital and fuel costs and reduce operational flexibility. Toughness has been improved by lowering the Bs temperature through Ni additions and increasing the quench rate (i.e., oil quenching and tempering, as opposed to the standard fan cooling and tempering heat-treatment condition) and refining austenite grain size through the addition of 0.04 pct Nb.[71] Based on this work, production of a prototype rotor forging made to an HP composition with enhanced hardenability is planned. In addition to improving the startup and shutdown flexibility of standard high-pressure steam turbines, the new grade is expected to provide a longer service life and may also be applied to high-temperature–low-temperature combination property turbine rotors and gas turbine rotors.

C. 2.25Cr-1Mo Steel

A 150-metric-ton ingot of HP 2.25Cr-1Mo, modified with additions of V for improved creep strength, B for enhanced hardenability, and Ti for gettering the residual

nitrogen, has been cast, forged into a prototype shell forging, heat treated, and evaluated for mechanical properties.[72] The new grade reportedly has improved temper embrittlement resistance and similar creep rupture properties to that of the standard grade. The new steel is planned to be used in coal liquefication applications in Japan.

V. CONCLUSIONS/ALLOY DESIGN GUIDELINES

Based on our studies of Mn, Si, and impurities, the following conclusions have been drawn, which have led to the development of some guidelines for the design of high-temperature bainitic steels.

1. Charpy impact toughness, fracture toughness, and tensile ductility are enhanced by increasing the level of microcleanliness in the steels. This can be accomplished through reductions in both S and Mn contents. However, additional austenite grain coarsening may occur in nonmicroalloyed steels (*i.e.*, without austenite grain refiners such as V, Nb, and Ti) as the microcleanliness is improved. Hence, microalloying may also be required to compensate for the loss in austenite grain refinement.
2. Toughness is improved by minimizing the susceptibility of the steels to temper embrittlement. This is accomplished primarily by lowering the P, Mn, and Si contents in the steels in accordance with the *J* factor relationship. A secondary contributor to temper embrittlement was found to be the steel's Sn + As + Sb contents. However, commercial levels of Sn + As + Sb may still offer adequate temper embrittlement resistance in an HP-type composition.
3. The HP-type steels are not susceptible to overheating at temperatures up to at least 1400 °C. Hence, these steels can be hot-worked at higher temperatures, thus reducing deformation loads and possibly the number of reheating cycles (*e.g.*, as required in the open-die forging of a turbine rotor).
4. When HP-type steels are designed, the Ac_1 and Ac_3 temperatures should be examined in order to assess the need for adjustments in the tempering and austenitizing temperatures, respectively.
5. A reduction in the Mn content or an increase in the Si content in bainitic steels results in a reduction in hardenability. The *Bs* temperature equation can be used to compensate for the loss in hardenability when lowering the Mn level through additions of alloying elements such as Ni, Cr, or Mo.
6. Tempering resistance may be reduced by lowering the Si content in these steels. As a result, adjustment of the tempering treatment may be required to achieve the desired strength level.
7. Creep rupture strength is improved by reducing Mn content, presumably due to the presence of a larger volume fraction of tempered upper bainite, which contains a more uniform dispersion of fine, creep strength-controlling carbonitrides. Creep ductility is also improved when the Si content of the steel is reduced.
8. The low-cycle fatigue behavior of the bainitic steels

is unaffected by variations in Mn, Si, and impurity contents.

VI. SUMMARY

In summary, there are many advantages to producing "clean steels" which contain low levels of Mn, Si, and impurities. Such steels have been shown to exhibit improved toughness, ductility, temper embrittlement resistance, creep rupture strength, creep rupture ductility, and overheating resistance. In addition, these steels have been shown to be commercially producible. On the negative side, such steels may exhibit a loss in hardenability and temper resistance as well as greater austenite grain coarsening. Fortunately, these negative aspects of the clean steels can be easily overcome by alloying to compensate for hardenability loss, adjusting the tempering heat treatment, and microalloying for austenite grain refinement, respectively.

REFERENCES

1. W. Steven and K. Balajiva: *J. Iron Steel Inst.*, 1959, vol. 193, pp. 141-47.
2. L.F. Porter, G.C. Carter, and S.J. Manganello: in *Temper Embrittlement in Steel*, ASTM STP 407, ASTM, Philadelphia, PA, 1968, pp. 20-45.
3. G.C. Gould: in *Temper Embrittlement in Steel*, ASTM STP 407, ASTM, Philadelphia, PA, 1968, pp. 59-73.
4. P. Opel, C. Florin, F. Hochstein, and K. Fischer: *Stahl Eisen*, 1970, vol. 90, pp. 465-75.
5. R. Bruscato: *Weld. J.*, 1970, vol. 49, pp. 148s-56s.
6. A. Joshi, P.W. Palmberg, and D.F. Stein: *Metall. Trans. A*, 1975, vol. 6A, pp. 2160-61.
7. P.E. Reynolds, J.H. Reynolds, and D. Dulieu: in *Proc. 7th Int. Forging Conf.*, Paris, 1975, paper no. 11, pp. 1-18.
8. C.L. Briant, H.C. Feng, and C.J. McMahon: *Metall. Trans. A*, 1978, vol. 9A, pp. 625-33.
9. I. Olefjord: *Int. Metals Rev.*, 1978, vol. 23 (4), pp. 149-63.
10. J. Yu and C.J. McMahon, Jr.: *Metall. Trans. A*, 1980, vol. 11A, pp. 291-300.
11. C.J. McMahon, Jr., S. Takayama, T. Ogura, S.-C. Fu, J.C. Murza, W.R. Graham, A.C. Yen, and R. DiDio: EPRI Report NP-1501, Sept. 1980.
12. J.C. Murza and C.J. McMahon, Jr.: *J. Eng. Mater. Tech.*, Trans. ASME, 1980, vol. 102, pp. 369-75.
13. J.F. Smith: *Acta Metall.*, 1980, vol. 28, pp. 1555-64.
14. P.E. Reynolds, J.H. Reynolds, and D. Dulieu: in *Proc. 9th Int. Forging Conf.*, Düsseldorf, Federal Republic of Germany, 1981, pp. 2.4.1-2.4.27.
15. Y. Takeda and C.J. McMahon, Jr.: *Metall. Trans. A*, 1982, vol. 13A, pp. 111-16.

16. R. Viswanathan and R.I. Jaffee: *J. Eng. Mater. Tech.*, Trans. ASME, 1982, vol. 104, pp. 220-26.
17. J.F. Smith, J.H. Reynolds, and H.N. Southworth: *Metal Sci.*, 1982, vol. 16, pp. 431-34.
18. C.J. McMahon, Jr., J.C. Murza, and D.H. Gentner: *J. Eng. Mater. Tech.*, Trans. ASME, 1982, vol. 104, pp. 241-48.
19. C.L. Briant and S.K. Banerji: in *Treatise on Materials Science and Technology, Vol. 25, Embrittlement of Engineering Alloys*, C.L. Briant and S.K. Banerji, eds., Academic Press, New York, NY, 1983, pp. 21-58.
20. Q. Zhe, Y.Q. Weng, S.-C. Fu, and C.J. McMahon, Jr.: EPRI Report CS-3248, Nov. 1983.
21. R.I. Jaffee: *Metall. Trans. A*, 1986, vol. 17A, pp. 755-75.
22. R.L. Bodnar and R.F. Cappellini: in *MiCon 86: Optimization of Processing, Properties, and Service Performance Through Microstructural Control*, ASTM STP 979, B.L. Bramfitt, R.C. Benn, C.R. Brinkman, and G.F. Vander Voort, eds., ASTM, Philadelphia, PA, 1988, pp. 47-82.
23. S. Tanimoto, I. Kitagawa, and S. Watanabe: in *Advances in Material Technology for Fossil Power Plants*, R. Viswanathan and R.I. Jaffee, eds., ASM INTERNATIONAL, Metals Park, OH, 1987, pp. 89-96.
24. Weng Yu-qing and C.J. McMahon, Jr.: *Proc. 4th JIM Int. Symp. on Grain Boundary Structure and Related Phenomena*, Minakami, Gunma Prefecture, Japan, Nov. 25–29, 1985, printed in *Suppl. to Trans. JIM*, 1986, vol. 27, pp. 579-85.
25. H.J. Grabke, K. Hennesen, R. Möller, and W. Wei: *Scripta Metall.*, 1987, vol. 21, pp. 1329-34.
26. J. Watanabe and Y. Murakami: American Petroleum Institute, 1981, preprint no. 28-81, pp. 216-24.
27. R.A. Swift: in *Applications of 2-1/4Cr-1Mo Steel for Thick-Wall Pressure Vessels*, ASTM STP 755, G.S. Sangdahl and M. Semchyshen, eds., ASTM, Philadelphia, PA, 1982, pp. 166-88.
28. T. Sekine, Y. Kusuhara, N. Ohashi, S. Ueda, S. Sato, T. Enami, and S. Sato: Kawasaki Steel Corporation Report, May 1980.
29. B.J. Shaw: presented at the 46th Midyear Rejoining Meeting of the American Petroleum Institute, Chicago, IL, May 1981, preprint no. 29-81.
30. G.E. Danner and E. Dyble: *Metal Progress*, 1961, vol. 79, pp. 75-78.
31. J. Comon: in *Proc. 6th Int. Forging Conf.*, Cherry Hill, NJ, 1972, pp. 1-18.
32. S. Sawada, K. Suzuki, and J. Watanabe: in *Proc. 98th Winter Annual Meeting*, ASME, New York, NY, 1977, pp. 89-106.
33. T. Fujii, D.R. Poirier, and M.C. Flemings: *Metall. Trans. B*, 1979, vol. 10B, pp. 331-39.
34. J. Menglong: *Iron and Steel*, 1979, vol. 14 (6), pp. 13-21 (BISI Translation 1981).
35. K. Suzuki and K. Taniguchi: *Trans. ISIJ*, 1981, vol. 21, pp. 235-42.
36. A. Suzuki: in EPRI WS-79-235, Sept. 1981, pp. 4-95-4-103.
37. S. Sawada and S. Kawaguchi: in EPRI WS-79-235, Sept. 1981, pp. 5-1-5-14.
38. H. Yamada, T. Sakurai, T. Takenouchi, and K. Suzuki: TMS-AIME Paper No. A82-30, 1982, pp. 1-5.
39. J.J. Moore and N.A. Shah: *Int. Metals Rev.*, 1983, vol. 28 (6), pp. 338-56.
40. J.T. Kim, M.R. Pyo, Y.S. Chang, and H.S. Chang: in *Steel Forgings*, ASTM STP 903, E.G. Nisbett and A.S. Melilli, eds., ASTM, Philadelphia, PA, 1986, pp. 45-56.
41. V.P. Swaminathan, R.I. Jaffee, and J.E. Steiner: in *Steel Forgings*, ASTM STP 903, E.G. Nisbett and A.S. Melilli, eds., ASTM, Philadelphia, PA, 1986, pp. 124-42.
42. J.E. Steiner, P.E. Busby, R.I. Jaffee, E.L. Murphy, D.L. Newhouse, and H.A. Wriedt: EPRI Report RD-3336, Dec. 1983.
43. J.E. Steiner and R.I. Jaffee: in *Steel Forgings*, ASTM STP 903, E.G. Nisbett and A.S. Melilli, eds., ASTM, Philadelphia, PA, 1986, pp. 35-44.
44. T. Ohhashi, R.L. Bodnar, H.S. Reemsnyder, and R.E. Steigerwalt: EPRI Report NP-5399, Sept. 1987.
45. G.E. Hale, S. Preston, and J. Nutting: *Mater. Sci. and Eng.*, 1986, vol. 2, pp. 571-75.
46. E.T. Turkdogan, S. Ignatowice, and J. Pearson: *JISI*, 1955, vol. 180, pp. 349-54.
47. G.E. Hale and J. Nutting: *Int. Metals Rev.*, 1984, vol. 29 (4), pp. 273-98.
48. R.L. Bodnar, K.A. Taylor, K.S. Albano, and S.A. Heim: in *29th Mechanical Working and Steel Processing Conf. Proc.*, Iron and Steel Society–AIME, 1988, vol. 25, pp. 157-69.
49. K.W. Andrews: *JISI*, 1965, vol. 203, pp. 721-27.
50. K.A. Abiko, R.L. Bodnar, and D.P. Pope: in *Ductility and Toughness Considerations in Elevated Temperature Service*, G.V. Smith, ed., ASME, New York, NY, 1978, pp. 1-10.
51. W. Steven and A.G. Haynes: *JISI*, 1956, vol. 183, pp. 349-59.
52. R.L. Bodnar, R.F. Cappellini, and R.I. Jaffee: *Ironmaking and Steelmaking*, 1987, vol. 14 (4), pp. 185-94.
53. E.C. Bain and H.W. Paxton: *Alloying Elements in Steel*, 2nd ed., ASM, Metals Park, OH, 1966, pp. 192-95.
54. S.J. Barnard, G.D.W. Smith, A.J. Garratt-Reed, and J. Vander Sande: in *Advances in the Physical Metallurgy and Applications of Steels*, TMS, London, 1982, pp. 33-37.
55. V.P. Swaminathan and J.D. Landes: in *Fracture Mechanics: 15th Symp.*, ASTM STP 833, R.J. Sanford, ed., ASTM, Philadelphia, PA, 1984, pp. 315-32.
56. M. Kohno, M. Ikuta, M. Miyakawa, and S. Kinoshita: *Trans. ISIJ*, 1987, vol. 27, p. B-25.
57. M. Kohno, M. Miyakawa, S. Kinoshita, and A. Suzuki: in *Advances in Material Technology for Fossil Power Plants*, R. Viswanathan and R.I. Jaffee, eds., ASM INTERNATIONAL, Metals Park, OH, 1987, pp. 81-88.
58. M. Miyakawa, M. Kohno, S. Kinoshita, H. Kikuchi, and A. Suzuki: in *1st Int. Conf. on Improved Coal-Fired Power Plants*, A. Armor, W. Bakker, R.I. Jaffee, and G. Touchton, eds., EPRI Publication CS-5581-SR, 1988, pp. 6-217-6-231.
59. H.G.A. Bates and K.A. Ridal: in *Joint Int. Conf. on Creep*, Inst. Mech. Eng., London, 1963, paper no. 72, pp. 1-99-1-113.
60. G.J.P. Buchi, J.H.R. Page, and M.P. Sidey: *JISI*, 1965, vol. 203, pp. 291-97.
61. J.F. Norton and A. Strang: *JISI*, 1969, vol. 207, pp. 193-203.
62. R.M. Magdowski and M.O. Speidel: *Metall. Trans. A*, 1988, vol. 19A, pp. 1583-96.
63. R.I. Jaffee, P. Machner, W. Meyer, and J.E. Steiner: *Ironmaking and Steelmaking*, 1986, vol. 13 (6), pp. 322-26.
64. P. Machner, E. Reisl, W. Meyer, and R.I. Jaffee: Final Report to EPRI, RP2741-3, Nov. 1986.
65. P. Machner, W. Meyer, A. Kucharz, and R.I. Jaffee: in *Clean Steel 3*, The Institute of Metals, London, 1987, pp. 168-72.
66. O. Watanabe and S. Ganesh: in *1st Int. Conf. on Improved Coal-Fired Power Plants*, A. Armor, W. Bakker, R.I. Jaffee, and G. Touchton, eds., EPRI Publication CS-5581-SR, 1988, pp. 6-41-6-58.
67. O. Watanabe, Y. Yoshioka, and R.C. Schwant: presented at the EPRI Workshop on Fossil Plant Retrofits for Improved Heat Rate and Availability, San Diego, CA, Dec. 1–3, 1987.
68. R.I. Jaffee, T. Ohhashi, O. Watanabe, and P. Machner: presented at the *Iron & Steel Society–AIME's 29th Mechanical Working and Steel Processing Conf.*, Toronto, ON, Canada, Oct. 21–23, 1987; and published in *Iron and Steelmaker*, 1989, vol. 16 (2), pp. 45-51.
69. A. Suzuki: Kobe Steel, Ltd., private communication, Jan. 1988.
70. Y. Takeda: Mitsubishi Heavy Industries, Ltd., private communication, Aug. 1987.
71. R.L. Bodnar, J.R. Michael, S.S. Hansen, and R.I. Jaffee: in *30th Mechanical Working and Steel Processing Conf. Proc.*, Iron and Steel Society–AIME, 1989, vol. 26, pp. 173-94.
72. J. Watanabe: Japan Steel Works, Ltd., private communication, April 1987.